Predicting Harmful Algal Blooms Using Explainable Deep Learning Models: A Comparative Study

Bekir Zahit Demiray[1], Omer Mermer[1], Özlem Baydaroğlu[1], Ibrahim Demir[1,2,3]

[1] IIHR—Hydroscience and Engineering, University of Iowa, Iowa City, Iowa, USA
[2] Civil and Environmental Engineering, University of Iowa, Iowa City, Iowa, USA
[3] Electrical and Computer Engineering, University of Iowa, Iowa City, Iowa, USA

* Corresponding Author: bekirzahit-demiray@uiowa.edu

Abstract

Harmful algal blooms (HABs) have emerged as a significant environmental challenge, impacting aquatic ecosystems, drinking water supply systems, and human health due to the combined effects of human activities and climate change. This study investigates the performance of deep learning models, particularly the Transformer model, as there are limited studies exploring its effectiveness in HAB prediction, considering multiple influencing parameters including physical, chemical, and biological water quality monitoring data from multiple stations located west of Lake Erie, and uses Shapley Additive Explanations (SHAP) values as an explainable artificial intelligence (AI) tool to identify key input features affecting HABs. Our findings highlight the superiority of deep learning models, especially the Transformer, in capturing the complex dynamics of water quality parameters and providing actionable insights for ecological management. The SHAP analysis identifies particulate organic carbon, particulate organic nitrogen, and total phosphorus as critical factors influencing HAB predictions. This study contributes to the development of advanced predictive models for HABs, aiding in early detection and proactive management strategies.

Keywords: Harmful Algal Bloom (HAB), prediction, deep learning, transformer, chlorophyll-a, water quality, explainable ai, SHAP value.

1. Introduction

The emergence and proliferation of Harmful Algal Blooms (HABs), particularly characterized by cyanobacteria, also known as blue-green algae, have escalated into a pressing environmental issue affecting water bodies worldwide. These blooms significantly impact water quality, public health, and the balance of aquatic ecosystems (Demir et al., 2009). The primary culprits behind the surge in HAB incidents include nutrient pollution, primarily from agricultural production and industrial waste, coupled with climatic variables such as rising water temperatures and altered water quality characteristics (Paerl and Paul, 2012; Graham et al., 2016). HABs are notorious for producing dangerous toxins, undermining the aesthetic and recreational value of waterways, and challenging the provision of clean drinking water (Weirich and Miller, 2014). The situation is further exacerbated by the dramatic rise in HAB events in recent years, attributed to the rapid expansion of human populations, extensive agricultural practices, escalating pollution levels, and the overarching effects of climate change (Yeşilköy and Demir, 2024; Tanir et al., 2024).

This disturbing trend underscores the urgent need for the development and refinement of HAB monitoring, estimation, modeling, and prediction techniques to protect water resources and public health (Greene et al., 2021; Ratté-Fortin et al., 2023; Paerl et al., 2016; Yan et al., 2024a). Given these challenges, it becomes imperative to monitor and develop forecasting tools for HABs, to ensure public health and safety. However, direct measurement of algal concentrations is labor-intensive and time-consuming, where the chlorophyll-a concentration often serves as a proxy for algal blooms (Boyer et al., 2009) and poor water quality (Mellios et al., 2020). Therefore, it would be desirable to predict the occurrence of HABs from other readily measured variables that are primary factors contributing to the proliferation of HABs.

HABs formation typically results from a combination of factors that create a favorable growth environment (Wells et al., 2015). Key contributors to HABs include eutrophication, deteriorating water quality—especially high levels of nitrogen and phosphorus—and climate change (Glibert, 2020; Zhou et al., 2022a). Over the last few decades, numerous studies have focused on the effects of individual factors like nutrients, land use or climate drivers on HABs, rather than examining the complex interaction of physical, chemical, and biological factors (Wells et al., 2020; Maze et al., 2015; Paerl et al., 2011). However, these studies often relied on single data related to the individual factors, leading oversimplified prediction, and potential errors. Therefore, the harmful effects of HABs on ecosystems, the economy, and public health require understanding the complex interrelation between triggering HABs and their strict monitoring.

Effective monitoring of HABs often requires laboratory analysis of water samples to assess a variety of indicators such as chlorophyll-a (Katin et al., 2021), cyanobacteria (Giere et al., 2020), and various algal toxins (Greer et al., 2016). The laboratory techniques used for these analyses encompass microscopy, spectrophotometry, liquid chromatography, and biochemical assays (Lombard et al., 2019). Such techniques are vital for identifying algae at the species level and require specialized technical expertise. Additionally, the use of remote sensing derived data from satellites and UAVs provides valuable spatial information of HAB spread (Rolim et al., 2023; Kislik et al., 2022; Cheng et al., 2020; Qui et al., 2023), making it easier to observe bloom

conditions across different water bodies. Addressing the issue of algal blooms and their harmful effects necessitates a thorough understanding of their causes and the implementation of effective management strategies, including timely prediction of HAB. Consequently, ensuring the accuracy of HAB predictions is crucial for effectively responding to this global environmental challenge and safeguarding both the ecological environment and human health (Beck et al., 2010).

There are various prediction models in the literature addressing the HABs. Physical process-based models (Shin et al., 2019; Verhamme et al., 2016; Wynne et al., 2013; Baek et al., 2021) specify physical and biochemical processes that influence HABs. Typical physical process-based models include Environmental Fluid Dynamic Code (EFDC), Water Quality Analysis Simulation (WASP), QUAL2K (Bui et al., 2019; Zheng et al., 2021; Wool et al., 2020; Demir and Beck, 2009). While these models have high prediction accuracy with complete data, constructing perfect data, particularly with spatial resolution, is costly and involves practical limitations. In addition to process-based models, statistical models, which use formula or fits to correlate various variables (physicochemical, meteorological, and hydrodynamic) to HAB indicators, sometimes struggle to capture complex nonlinear relationships and lack predictive accuracy (Liu and Zhang, 2022; Baydaroğlu et al., 2024; Franks et al., 2018). Both approaches have their contributions to studying HAB dynamics but often encounter limitations in accurately capturing complex interactions and maintaining predictive accuracy under varied conditions (Janssen et al., 2019).

Due to limitations of these traditional physical and statistical models, data-driven models have emerged as ideal alternatives and have recently gained popularity being applied to solve various problems in hydrology and atmospheric studies (Sit et al., 2024; Baydaroğlu and Demir, 2024), environmental monitoring (Demiray et al., 2023), environmental management (Tounsi et al., 2023; Wang et al., 2019; Bayar et al., 2009). Similarly, recent applications of these models have focused on predicting HABs by analyzing the relationship between various algal-related factors and water quality parameters (Chen et al., 2023; Yan et al. 2024b; Rostam et al., 2023). Various machine learning (ML) models have been developed and are in practice for determining drivers of algal dynamics and multistep prediction in various lakes, rivers, and reservoirs (Busari et al., 2024; Ai et al., 2023; Lin et al., 2023; Jeong al., 2022; Izadi et al., 2021; Derot et al., 2020).

Among them, Ai et al. (2023) presented a comprehensive study to compare the performance of widely used ML algorithms, including bootstrap aggregating (BA), gradient boosting (GB), gaussian processes (GP), k-nearest neighbors (KNN), Random Forrest (RF), support vector machine (SVM), and XGBoost (XGB), for predicting HABs. In addition to these algorithms, Yu et al. (2021) used Adaptive Boosting (AdaBoost), Gradient Boosting Decision Tree (GBDT) algorithms to predict HAB occurrence. However, limited information is available on criteria for selecting, validating, and evaluating the performance of ML models for HAB prediction (Busari et al., 2023). Besides these ML models, researchers have also applied deep learning (DL) models which have recently gained popularity due to their significant advantages such as the ability to capture temporal dynamics and handle complex interactions among features effectively (Demiray et al., 2021; Sit et al., 2021a).

For example, several studies performed HAB prediction using different Long-Short Term Memory (LSTM) based models (Lee and Lee, 2018; Hu et al., 2019; Marndi et al., 2020; Yussof et al., 2021). Lee at al. (2022) used and compared integrated CNN model and LSTM to predict HABs for multiple streams from 29 stations in four South Korean rivers and showed that prediction performance for all monitoring stations of integrated CNN model was better than LSTM based models. In addition, a few recent studies have used the state-of-the-art DL algorithms such as Gated Recurrent Unit (GRU) and the Transformer for water quality prediction (Busari et al, 2024; Qian et al., 2023). Despite studies to predict HABs via ML/DL models is increasing, making optimal HAB predictions by reflecting various parameters, time series characteristics and performance evaluation remains challenging.

Developing accurate predictive models necessitates thorough research into specific algal-related factors and water quality parameters that significantly affect HAB dynamics. Parameters such as particulate organic matter, total phosphorus, dissolved phosphorus and turbidity play crucial roles in influencing chlorophyll-a concentrations in lakes and ponds (Du et al., 2022; Zhou et al., 2017; Wang et al., 2011). Chlorophyll-a is a vital indicator of HABs, with its distribution and concentration closely linked to algal growth and toxicity (Humbert and Fastner, 2016). Although the growth of cyanobacteria often correlates with increased chlorophyll-a levels, their toxicity can vary based on specific environmental factors at different sites (Hartshorn et al., 2016), indicating a more complex relationship between chlorophyll-a and algal toxins. Furthermore, higher chlorophyll-a concentrations do not always signify high toxin levels but may indicate a higher probability of exceeding certain thresholds (Hollister and Kreakie, 2016). Therefore, understanding the main drivers of HABs remains pivotal for accurate prediction and prevention efforts.

In addition, all the data driven models previously discussed exhibit black box characteristics. This implies that the end user has access only to the input information provided in the models (Saeed and Omlin, 2023). Consequently, decision-makers are often unaware of the reasoning behind the predictions made by complex AI systems. To tackle these issues, concepts such as explainable AI have been developed (Arrieta et al., 2020). Explainable AI aims to create methodologies that enable human stakeholders to understand and interpret artificial systems (Langer et al., 2021). The sophistication of AI-based systems has advanced to a level where human intervention is seldom necessary for their design and deployment.

However, when decisions made by such systems impact human lives, particularly in fields like medicine and law, it becomes crucial to comprehend how these decisions are generated by AI methods (Goodman and Flaxman, 2017). While early AI systems were relatively interpretable, the rise of deep learning has introduced models with an enormous number of parameters, rendering their outputs difficult to explain—a concept known as black-box properties (Castelvecchi, 2016). Most deep learning models (such as LSTM, CNN, RNN) used to predict algal bloom possess deep layers with numerous parameters, exhibiting the black-box property and predicting only singular pieces of information. Given that algal bloom is influenced by a multitude of variables and exhibit

nonlinear growth patterns, understanding the contribution of each variable in predicting the target variable is essential.

Lake Erie, part of the Great Lakes system, serves as a critical case study for examining HABs. The Great Lakes constitute the largest and most biodiverse freshwater reserve on Earth (Magnuson et al., 1997; Tewari et al., 2022). The Great Lakes basin encompasses both industrial facilities focused on manufacturing and areas dedicated to agriculture. Among the Great Lakes, Lake Erie is the shallowest, smallest lake in terms of water volume, and the fourth largest in terms of area. It is ecologically, culturally, and economically significant to the approximately 12.5 million people who live in its watershed. Each year Lake Erie supports nearly 14,000 tons of commercial and traditional fisheries, over 33 million tons of freight, and over USD 1.5 million in recreation and tourism business (Sterner et al., 2020). It experiences significant impacts from nutrient overload, especially from its western basin due to its geographical location (Boegehold et al., 2023).

Since 2002, chlorophyll-a concentration, an accepted indicator of eutrophication and HABs, has dramatically increased annually in Lake Erie, reaching unprecedented levels in recent years (Stumpf et al., 2016; Boegehold et al., 2023). Humans can be exposed to harmful algae through ingestion of contaminated fish and drinking water and through inhalation and dermal exposure during recreational events such as swimming and boating (Carmichael and Boyer, 2016; Buratti et al., 2017). Given the risks HABs pose to human health, the economy, and the environment, accurate prediction of HAB occurrences is essential. Identifying key factors influencing these blooms is crucial for implementing preventive measures to mitigate potential losses (Kouakou and Poder, 2019).

Despite human and ecological health risks associated with HABs, there is a lack of holistic understanding of factors influencing HABs. Previous studies have been conducted using field measurements and statistical methods or machine learning techniques to predict HABs for Lake Erie. Additionally, while existing research has only focused on HAB prediction performance, few studies have identified the effect of each variable on the target variable chlorophyll-a in HABs prediction. Furthermore, there is a lack of studies that have conducted comparative testing of deep learning model performance, specifically regarding time-series data and in-depth interpretations by explainable AI approach (XAI).

To address these gaps, we investigated the performance of deep learning models, particularly the Transformer model, as there are limited studies exploring their effectiveness in HAB prediction, considering multiple influencing parameters including physical, chemical, and biological water quality monitoring data from multiple stations located west of Lake Erie, and used SHAP (SHapley Additive exPlanations) values as an explainable AI tool to identify key input features affecting HABs. Addressing gaps in prior research, in summary, this study aims to: (1) utilize comprehensive datasets that encompass physical, chemical, and biological water quality parameters from multiple monitoring stations; (2) evaluate and compare the performance of various deep learning models, with a particular emphasis on the Transformer model, for predicting HABs in Lake Erie; (3) uncover significant features influencing HABs formation.

We anticipate that this study (model comparison with indices) will aid scientists and stakeholders in understanding HAB formation mechanisms and serve as a practical reference, theoretical guide, and potential prediction standard for protecting ecosystems globally. This paper is organized as follows: Section 2 introduces the dataset utilized in this study. Section 3 details the methods tested, their specifications, and the role of explainable artificial intelligence (XAI). Section 4 presents the results and discussion, emphasizing the role of SHAP in interpreting the models. Finally, Section 5 concludes with insights into the implications of our findings and offers suggestions for future research directions.

2. Study Area and Dataset

As nutrient load and HAB occurrence predominantly affect the western part of Lake Erie, this study focused on the western basin of Lake Erie, which includes the area from the western part of the lake to Point Pelee, ON, Canada, and Cedar Point, OH, USA (shown in Fig. 1). Water quality data, collected from seven monitoring stations (Fig. 1) on the U.S. side of the western part of Lake Erie and operated by the National Oceanic and Atmospheric Administration (NOAA) Great Lakes Environmental Research Laboratory (GLERL), was used. This dataset encompasses water quality measurements sampled from 2013 to 2020 (Boegehold et al., 2023).

These stations are selected to represent the various nutrient and sediment inputs into the western basin of Lake Erie and highlight areas consistently susceptible to HABs. The selected water quality parameters measured at these stations included Secchi Depth (m), CTD Temperature (°C), CTD Specific Conductivity (µS/cm), CTD Dissolved Oxygen (mg/L), Turbidity (NTU), Total Phosphorus (µg P/L), Total Dissolved Phosphorus (µg P/L), Ammonia (µg N/L), Nitrate + Nitrite (mg N/L), Particulate Organic Carbon (mg/L), Particulate Organic Nitrogen (mg/L), Total Suspended Solids (mg/L), and Chlorophyll-a (µg/L). The primary objective was to predict chlorophyll-a concentration as a key indicator of HABs.

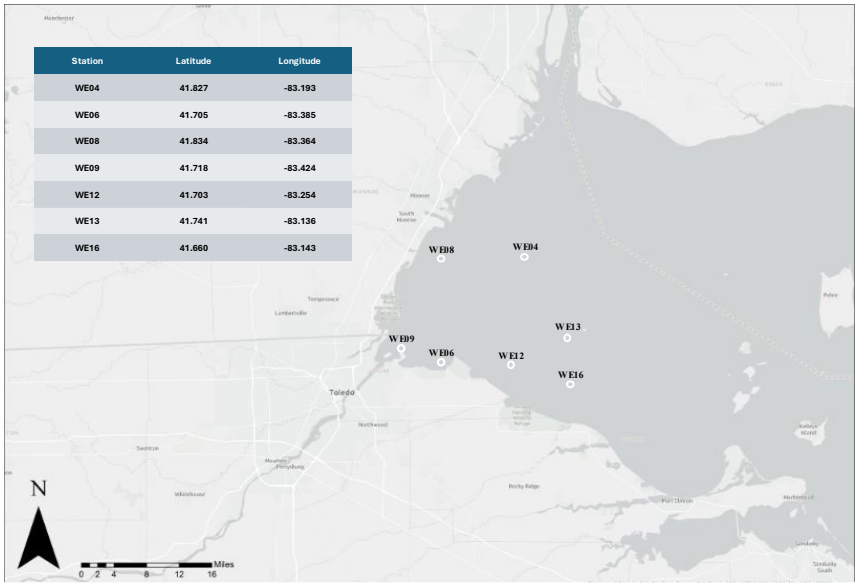

Figure 1. Location and description western Lake Erie water quality monitoring stations.

Table 1 presents a summary of the descriptive statistics of the complete dataset after pre-processing. Particulate Organic Carbon and Particulate Organic Nitrogen levels exhibited considerable variation, with maximum values far exceeding the averages, indicating the presence of organic matter in differing concentrations throughout the samples. Similarly, Total Suspended Solids and Chlorophyll-a showed large ranges in value, reflecting varied conditions in the sampled water bodies. The standard deviation for each variable highlights the extent of variability in the measurements, with certain variables such as turbidity and total phosphorus displaying significant variability.

Table 1. Descriptive statistical summary of used dataset

Variables	**Min**	**Max**	**Mean**	**Median**	**Std. Dev**
Secchi Depth (m)	0.00	6.50	1.15	0.90	0.917
CTD Temperature (°C)	2.90	29.70	22.02	22.90	3.880
CTD Specific Conductivity (µS/cm)	19.90	583.30	297.76	280.40	67.028
CTD Dissolved Oxygen (mg/L)	4.20	13.04	7.58	7.60	1.148
Turbidity (NTU)	0.68	1148.00	19.76	9.30	55.561
Total Phosphorus (µg P/L)	4.00	2482.24	77.83	48.14	132.919
Total Dissolved Phosphorus (µg P/L)	0.16	273.58	20.42	9.27	28.248
Ammonia (µg N/L)	0.04	2108.70	33.61	12.25	87.502
Nitrate + Nitrite (mg N/L)	0.00	9.45	0.88	0.34	1.341
Particulate Organic Carbon (mg/L)	0.14	219.34	2.53	1.30	10.576
Particulate Organic Nitrogen (mg/L)	0.01	40.93	0.43	0.21	1.895
Total Suspended Solids (mg/L)	0.82	540.80	17.98	10.15	33.212
Chlorophyll-a (µg/L)	0.71	678.40	37.86	16.14	237.576

To prepare the dataset for modeling, the year 2020 was designated as the test set, while the remaining years were used for training purposes. From the training data, 20% was allocated as a validation set. Standard Scaler was applied to standardize the features, ensuring each feature had a mean of zero and a standard deviation of one. The dataset was converted into a time series format with a sequence length of three, meaning that each input sequence consisted of three consecutive time steps. One-hot encoding was used to specify each monitoring station, allowing the model to differentiate between data from different locations. To address the missing features in each input sequence provided to the models, the persistence method was employed (Demiray et al., 2024), which involves carrying forward the last known value.

3. Methods

This study evaluates the effectiveness of several machine models—Lasso, Ridge, LSTM, GRU, and Transformer—in forecasting harmful algal blooms (HABs) in Lake Erie. This section describes the setup and implementation of these models, providing insights into their application for HAB prediction.

3.1. Lasso and Ridge Regression Models

In predictive modeling, particularly when dealing with high-dimensional data, regularization techniques such as Lasso and Ridge regression are essential for managing multicollinearity and preventing overfitting. Both methods modify the least squares loss function by adding a penalty term, aiding in stabilizing the coefficients, though they do so in distinct ways. Lasso regression (Least Absolute Shrinkage and Selection Operator) applies a penalty equal to the absolute value of the coefficients, promoting sparsity within the model parameters. This L1 regularization helps in performing variable selection by reducing some coefficients to zero, which is particularly beneficial for enhancing model interpretability (Tibshirani, 1996). The formulation of the Lasso regression cost function (Eq. 1) is as follows:

$$L(w) = \frac{1}{2n}\sum_{i=1}^{n}(y_i - X_i w)^2 + \alpha\|w\|_1$$

$y_i = observation\ values$
$X_i = prediction\ values$
$w = vector\ of\ model\ coefficients$
$\alpha = regularization\ parameter$
$\|w\|_1 = the\ L1\ norm\ of\ the\ coefficients$

Eq.1

Conversely, Ridge Regression incorporates L2 regularization by adding a penalty equal to the square of the magnitude of the coefficients (Hoerl & Kennard, 1970). This approach does not lead to zero coefficients but reduces their size uniformly, helping to manage multicollinearity without excluding any variables. This method is formulated through the following cost function (Eq. 2):

$$R(w) = \frac{1}{2n}\sum_{i=1}^{n}(y_i - X_i w)^2 + \alpha\|w\|_2^2$$

$y_i = observation\ values$
$X_i = prediction\ values$
$w = vector\ of\ model\ coefficients$
$\alpha = regularization\ parameter$
$\|w\|_2^2 = the\ L2\ norm\ of\ the\ coefficients$

Eq.2

The selection between Lasso and Ridge often hinges on the data specifics and the analysis goals. While Lasso is favored for models that benefit from feature reduction, Ridge may be better suited for scenarios that require the retention of all features in a diminished capacity.

3.2. LSTM and GRU Models

Long Short-Term Memory (LSTM) and Gated Recurrent Units (GRU) are foundational to modern predictive modeling, especially noted for their efficiency in handling sequences and time-series

data. These models are designed to solve the problems inherent in traditional recurrent neural networks (RNNs), specifically the difficulty in learning long-range temporal dependencies.

LSTMs were introduced by Hochreiter and Schmidhuber in 1997 and have since become one of the most popular architectures for sequential data modeling due to their ability to maintain long-term dependencies. LSTM networks are composed of a series of units, each containing a cell state and various gates that regulate the flow of information. The key components of an LSTM unit are the cell state, forget gate, input gate, and output gate. The cell state is responsible for carrying information across different time steps and can be thought of as the memory of the network. The forget gate decides what information from the cell state should be discarded. It takes the previous hidden state and the current input and passes them through a sigmoid function. The input gate determines which new information should be added to the cell state. It comprises two parts: a sigmoid layer that decides which values to update and a tanh layer that creates a vector of new candidate values. The output gate decides what the next hidden state should be, which will be used in the next time step. It takes into account the current input, the previous hidden state, and the cell state. LSTMs have been widely applied in various domains, including natural language processing, speech recognition, and time series forecasting. Their ability to capture long-term dependencies makes them particularly suitable for tasks where context over extended sequences is important.

Gated Recurrent Units (GRUs) were introduced by Cho et al. in 2014 as a simplified variant of LSTMs. GRUs combine the forget and input gates into a single update gate and merge the cell state and hidden state, resulting in a more streamlined architecture. This simplification makes GRUs computationally more efficient while still retaining the capability to capture long-term dependencies. In a GRU, the update gate determines the amount of the previous hidden state that needs to be passed along to the future. This gate is computed using a sigmoid function that combines the previous hidden state and the current input. The reset gate, another key component of GRUs, decides how much of the past information to forget. It is also computed using a sigmoid function applied to the previous hidden state and the current input. The candidate hidden state is then calculated by applying a tanh function to the combination of the reset-modified previous hidden state and the current input. The final hidden state is obtained by linearly interpolating between the previous hidden state and the candidate hidden state using the update gate. GRUs have been found to perform comparably to LSTMs on many tasks, often with fewer parameters and less computational complexity. This makes them an attractive option for applications where computational resources are limited or where faster training times are desired.

Both LSTM and GRU architectures are adept at modeling environmental data, which is often non-linear and subject to sudden shifts due to underlying ecological dynamics. These models are versatile and have been employed in a variety of environmental studies (Sit et al., 2020), including streamflow forecasting (Kratzert et al., 2018), air quality prediction (Zhang et al., 2024), and water quality prediction (Liu et al., 2019). Each application showcases the ability of LSTM and GRU models to analyze and predict complex dynamic systems, making them invaluable tools in the field of environmental science.

These models have also been specifically applied in the context of harmful algal bloom (HAB) prediction (Lee et al., 2022; Busari et al., 2024), where their ability to process and make predictions based on diverse and dynamic environmental data inputs proves invaluable. By leveraging historical and current environmental data, they have demonstrated significant accuracy in predicting HABs, thereby supporting proactive management and mitigation strategies in water bodies. This practical application underlines the models' crucial role in not only understanding but also anticipating environmental changes that impact water quality and ecosystem health.

3.3. Transformer Model

The transformer model, originally introduced for natural language processing tasks (Vaswani et al., 2017), has demonstrated a remarkable ability to capture complex dependencies in sequential data. It represents a paradigm shift in sequential data modeling by leveraging self-attention mechanisms instead of recurrence, enabling them to handle long-range dependencies more efficiently. The core concept of the transformer model is the attention mechanism, which allows the model to weigh the importance of different elements within the input sequence dynamically.

The transformer architecture consists of an encoder-decoder structure. However, in this study, we employed an encoder-based transformer, which focuses on encoding the input sequence into a rich representation that captures temporal dependencies and interactions between various environmental factors. Typically, transformer models use an embedding layer to convert input elements into continuous vector representations. However, in our implementation, we used a linear layer as the embedding layer to convert each element of the input sequence into continuous embeddings. These embeddings are then processed by multiple layers of self-attention and feedforward neural networks.

The self-attention mechanism is the cornerstone of the transformer architecture. It allows the model to focus on different parts of the sequence simultaneously by computing attention weights over the entire sequence. The self-attention mechanism (Eq. 3) calculates a weighted sum of the input values, where the weights are determined by the relevance of each input element to others. This process is defined by the following equations:

$$Attention(Q, K, V) = softmax\left(\frac{QK^T}{\sqrt{d_k}}\right)V \qquad \text{Eq. 3}$$

where Q (queries), K (keys), and V (values) are the input embeddings, and d_k is the dimension of the keys. The attention mechanism computes the dot product of the queries and keys, scales it by the square root of the key dimension, and applies a softmax function to obtain the attention weights. These weights are then used to compute a weighted sum of the values, effectively allowing the model to focus on the most relevant parts of the sequence.

One of the innovative features of the transformer model is the multi-head attention mechanism, which enhances the self-attention mechanism by enabling the model to attend to information from different representation subspaces at different positions. Instead of performing a single attention

function, the multi-head attention mechanism projects the queries, keys, and values into multiple lower-dimensional spaces and performs the attention function in parallel. By attending to different parts of the sequence in parallel, the multi-head attention mechanism allows the model to capture a richer set of dependencies and interactions within the data.

Since the self-attention mechanism treats input sequences as sets without inherent order, positional encodings are added to the input embeddings to retain positional information, which is critical for sequence modeling tasks. These encodings use sine and cosine functions (Eq. 4) of different frequencies:

$$PE(pos, 2i) = \sin\left(\frac{pos}{10000^{2i/d_{model}}}\right)$$
$$PE(pos, 2i+1) = \cos\left(\frac{pos}{10000^{2i/d_{model}}}\right) \quad \text{Eq. 4}$$
$$pos = position$$
$$i = dimension$$

After the self-attention layers, the output is passed through a position-wise feedforward network, which applies two linear transformations with a ReLU activation in between. This network helps in learning complex patterns by introducing non-linearity and improving the model's expressiveness. The output of the feedforward network is then added to the input of that layer through a residual connection, followed by layer normalization, ensuring stable and efficient training.

Transformers have achieved state-of-the-art results in various domains, including natural language processing, machine translation, and more recently, time-series forecasting (Zhou et al., 2021; Wu et al., 2021; Zhou et al., 2022b; Demiray and Demir, 2024; Lin et al., 2022). Their ability to process entire sequences simultaneously rather than step-by-step as in RNNs or LSTMs makes them highly efficient, especially when dealing with long sequences. The Transformer model's architecture, leveraging self-attention mechanisms and positional encodings, can be a powerful tool for forecasting harmful algal blooms in Lake Erie. Its ability to capture complex temporal dependencies, handle large datasets, and offer explainable predictions makes it an invaluable asset in environmental monitoring and management. By enabling accurate and proactive HAB predictions, Transformers support efforts to protect water quality and ecosystem health, ultimately contributing to the sustainability of aquatic environments.

3.4. Specifications of Tested Models

The implementation of the models in this study was conducted using Python frameworks and libraries to ensure optimal performance and accuracy in forecasting HABs in Lake Erie. Each model's training environment was tailored through grid search to find the best hyperparameters, which varied across different models. For the Lasso and Ridge regression models, the scikit-learn library in Python was utilized. During the experiments, the maximum iteration parameter was set

to 100,000. The optimal alpha and tolerance values were found through grid search. Based on the experiments, for Lasso, the best solution was achieved with an alpha of 0.01 and a tolerance of 0.1, while for Ridge, the optimal alpha was 100 and the tolerance was 0.1.

The Long Short-Term Memory (LSTM), Gated Recurrent Units (GRU), and Transformer models were developed and tested using the PyTorch library. For all these models, the L1Loss function and Adam optimizer were used. During the training process, ReduceLROnPlateau and early stopping were employed. ReduceLROnPlateau is a learning rate scheduler that reduces the learning rate when a metric has stopped improving, helping to avoid plateaus during training. Early stopping is a technique used to stop training when the model's performance on a validation set stops improving, preventing overfitting. For the LSTM-based model, a linear layer was used at the beginning and end of the LSTM model, with dropout applied at the end. The training was set with 400 epochs for warm-up, 400 epochs for patience in ReduceLROnPlateau, and 1000 epochs for early stopping, with a learning rate of 0.001. The optimal solution was reached with a model consisting of two layers and a hidden dimension of 16, with a dropout rate of 0.

Similarly, for the GRU-based model, a linear layer was used at the beginning and end of the GRU, with a dropout layer at the end. The training configuration included 1000 epochs for warm-up, 100 epochs for patience, and 250 epochs for early stopping, with a learning rate of 1e-05. The optimal model had a hidden dimension of 32, four layers, and a dropout rate of 0.0. For the Transformer model, an encoder-based Transformer was used. The training setup included a learning rate of 0.001, 200 epochs for patience, 500 epochs for warm-up, and 500 epochs for early stopping. The model architecture included a linear layer as input embeddings. The Transformer used two attention heads, one layer, a model dimension (dmodel) of 128, a feedforward dimension of 64, and a dropout rate of 0.2. Positional encoding was tested but not used in the final model as it provided slightly lower performance. The results were very close, but since we used the models with the best MAE in other models, we followed the same criterion here as well.

The training process was performed on a machine equipped with NVIDIA GPUs to accelerate computation, particularly for the deep learning models. By utilizing grid search to tune hyperparameters, each model was optimized individually to achieve the best possible performance for HAB prediction. This approach acknowledges the unique requirements and strengths of each model, ensuring a fair and comprehensive comparison of their capabilities.

3.5. Model Interpretation Using XAI

Explainable Artificial Intelligence (XAI) aims to address one of the significant challenges in modern AI systems, particularly deep learning models: the lack of transparency and interpretability. As AI models, especially those based on deep learning, become more complex and widely used in critical applications such as environmental monitoring and public health, the ability to understand and trust the decisions made by these models becomes crucial.

In the context of predicting HABs, where decisions can significantly impact ecological management and public safety, the interpretability of models is not just a luxury but a necessity. Explainable models help stakeholders validate and trust the predictions, understand the

contributing factors leading to an event, and facilitate informed decision-making. This is particularly important in environmental science, where the interactions between numerous biotic and abiotic factors are complex and often non-linear.

To interpret the effects of water quality parameters on the predicted Chlorophyll-a concentrations by the deep learning models, SHAP (SHapley Additive exPlanations) was utilized. SHAP is a post-hoc, model-agnostic technique that unifies multiple interpretability methods under the concept of Shapley values (Lundberg et al., 2020; Stubblefield et al., 2020). It establishes a new explanatory model for a given black-box system by uncovering associations between feature values and the model's output (Burkart and Huber, 2021). This method is based on coalitional game theory and Shapley values, which represent a unique distribution of the total surplus generated by a coalition of all players in a cooperative game (Lundberg and Lee, 2017).

The GradientExplainer from the SHAP library was employed to estimate SHAP values. GradientExplainer is specifically designed for deep learning models and leverages the gradients of the model's output with respect to its inputs to compute SHAP values. These gradients help determine the importance of each input feature in predicting the model's output, providing insights into the decision-making process.

In the result section, feature importance was visualized using bar graphs representing the average absolute contribution of each feature, with larger values indicating higher importance. To provide both global and local interpretability, summary plots were created, showing the SHAP values of each feature for individual samples. By averaging these values over multiple predictions, it was possible to identify which features were generally important across the entire dataset. For individual predictions, the SHAP values explained why a specific outcome was reached, illustrating the contribution of each feature to that prediction. The relationship between the magnitude of a feature's value and the predicted outcomes was indicated by color coding in the summary plots, which also displayed the distribution of feature values. Positive SHAP values suggested that a feature contributed to an increase in Chlorophyll-a concentration, while negative SHAP values indicated a decrease.

By incorporating this XAI technique, the study aimed to bridge the gap between model performance and interpretability, ensuring that the predictive models for HABs were not only accurate but also understandable and actionable. This approach supports proactive management strategies for HAB mitigation, contributing to the sustainability of Lake Erie's ecosystem.

3.6. Performance Metrics

To evaluate the performance of HAB prediction models in Lake Erie, this study utilizes four key metrics: R-squared (R^2), Mean Absolute Error (MAE), Mean Absolute Percentage Error (MAPE), and Normalized Root Mean Square Error (NRMSE). These metrics were selected due to their effectiveness in capturing different aspects of model performance in environmental data modeling and are widely recognized in the field. Mean Absolute Error (MAE), Eq. 5, provides an intuitive and easily interpretable measure of prediction model performance. The MAE between the measured and predicted Chlorophyll-a concentrations is computed without considering their

direction. A lower MAE indicates a better model fit, showing that the model's predictions are closer to the true values. This metric is beneficial when comparing different models on the same dataset, as it helps identify the model with the most accurate predictions.

R-squared (R^2), Eq. 6, indicates how well the predictive value explains the measured value. In this work, measured and predicted Chlorophyll-a concentrations were taken as the dependent and independent variables, respectively, and R^2 was determined by applying linear regression analysis. The R^2 ranges from 0 to 1; the closer the value is to 1, the better the independent variable explains the dependent variable, meaning higher prediction accuracy. Mean Absolute Percentage Error (MAPE), Eq. 7, is another widely used performance metric that provides an intuitive and easily interpretable measure of prediction model performance. MAPE emphasizes relative errors and remains unaffected by overall scaling adjustments of the target variable. Smaller MAPE values indicate enhanced accuracy and stronger predictive capabilities of the model.

$$MAE = \frac{\sum_{i=1}^{n}|y_i - \hat{y}_i|}{n} \quad \text{Eq. 5}$$

$$R^2 = 1 - \frac{\sum_{i=1}^{n}(y_i - \hat{y}_i)^2}{\sum_{i=1}^{n}(y_i - \bar{y})^2} \quad \text{Eq. 6}$$

$$MAPE = \frac{1}{n}\sum_{i=1}^{n}\left|\frac{y_i - \hat{y}_i}{y_i}\right| \quad \text{Eq. 7}$$

$$NRMSE = \frac{\sqrt{\frac{\sum_{i=1}^{n}(y_i - \hat{y}_i)^2}{n}}}{\bar{y}} \quad \text{Eq. 8}$$

$y_i = actual\ value\ at\ time\ i$
$\hat{y}_i = predicted\ value\ at\ time\ i$
$n = number\ of\ sample$
$\bar{y} = mean\ of\ actual\ values$

The final metric used in this study is the Normalized Root Mean Square Error (NRMSE). NRMSE (Eq. 8) measures the average magnitude of the errors between the predicted and observed Chlorophyll-a concentrations, normalizing these errors against the mean of the observed data. This normalization provides a relative assessment of the model's accuracy, facilitating comparisons across different datasets. Due to the varying conditions and environmental factors in this study, NRMSE is an appropriate choice for evaluation. The metric ranges from 0 to 1, with lower values indicating better model performance by denoting smaller errors relative to the mean of the observed Chlorophyll-a concentrations. Higher NRMSE values indicate larger errors and reduced predictive accuracy, highlighting areas where the model may need improvement.

4. Results and Discussion

This section presents the findings from our comprehensive experiments aimed at developing predictive models for HABs using deep learning algorithms, with a focus on the relationship the

HAB indicator, chlorophyll-a, and various water quality parameters. The primary goal was to evaluate the predictive performance of five distinct models: Lasso, Ridge, LSTM, GRU, and Transformer. The Transformer model, with its innovative self-attention mechanism, represents a relatively recent advancement in this field and warrants a thorough examination for its potential in capturing complex temporal dependencies in environmental data.

We assessed each model's ability to predict Chlorophyll-a concentrations using four key metrics: R-squared, MAE, MAPE, and NRMSE. These metrics provide a comprehensive assessment of each model's predictive accuracy and effectiveness. Furthermore, we applied Explainable AI (XAI) technique, specifically SHAP value analysis, to enhance the interpretability of the models by identifying the contribution of different water quality parameters to the predictions. This combination of quantitative metrics and qualitative insights ensures a thorough evaluation of the models' capabilities in predicting HAB events and supports informed decision-making for ecological management and public safety.

We analyzed chlorophyll-a concentrations measured at seven stations from 2013 to 2020 on yearly (Figure 2a), monthly (Figure 2b), and station (Figure 2c) scale. These plots provide insight into the temporal and spatial variability of chlorophyll-a over the study period. The median chlorophyll-a concentration appears to fluctuate slightly over the years, with the highest median values observed in the earlier years, particularly between 2013 to 2015. However, significant outliers are present in nearly all years, with the highest concentrations recorded in 2015, indicating a substantial outbreak of HABs during this year. Notable peaks also occurred in 2019. In contrast, lover chlorophyll-a concentrations were recorded in years like 2016 and 2018. Based on month scale analysis, as shown in Figure 2b, the data indicates that high occurrences of HABs may occur in the period from late spring to early fall.

Specifically, from May to September, chlorophyll-a concentrations were substantially increased. This period often aligns with increased rainfall, which can lead to higher nutrient runoff from surrounding areas into the lake, thereby further elevating HABs. Finally, the spatial distribution of chlorophyll-a concentrations is shown in the station scale (Figure 2c), where data from seven monitoring stations (WE4, WE6, WE8, WE9, WE12, WE13, and WE16) are compared. Stations WE6, WE8 and WE9 (closest to the Maumee River inflow) consistently exhibit higher median chlorophyll-a concentrations, suggesting that these areas may be more prone to algal blooms, possibly due to localized nutrient inputs from river (Boegehold et al., 2023) compared to stations further out in the western basin of the lake (WE13 and WE16).

The results of our comprehensive experiments are summarized in Table 2. The comparative analysis of the models reveals distinct differences in their predictive performance. The Transformer model consistently outperformed the other models across all metrics, achieving the highest R-squared value and the lowest values for MAE, MAPE, and NRMSE. This indicates that the Transformer model is the most accurate and reliable for predicting HABs in Lake Erie among the tested models. The GRU model also demonstrated strong performance, closely following the Transformer. The GRU's simplified gating mechanism allows it to efficiently capture long-term dependencies, making it suitable for real-time monitoring and forecasting applications. This

balance between computational efficiency and predictive power makes it a robust choice for HAB prediction.

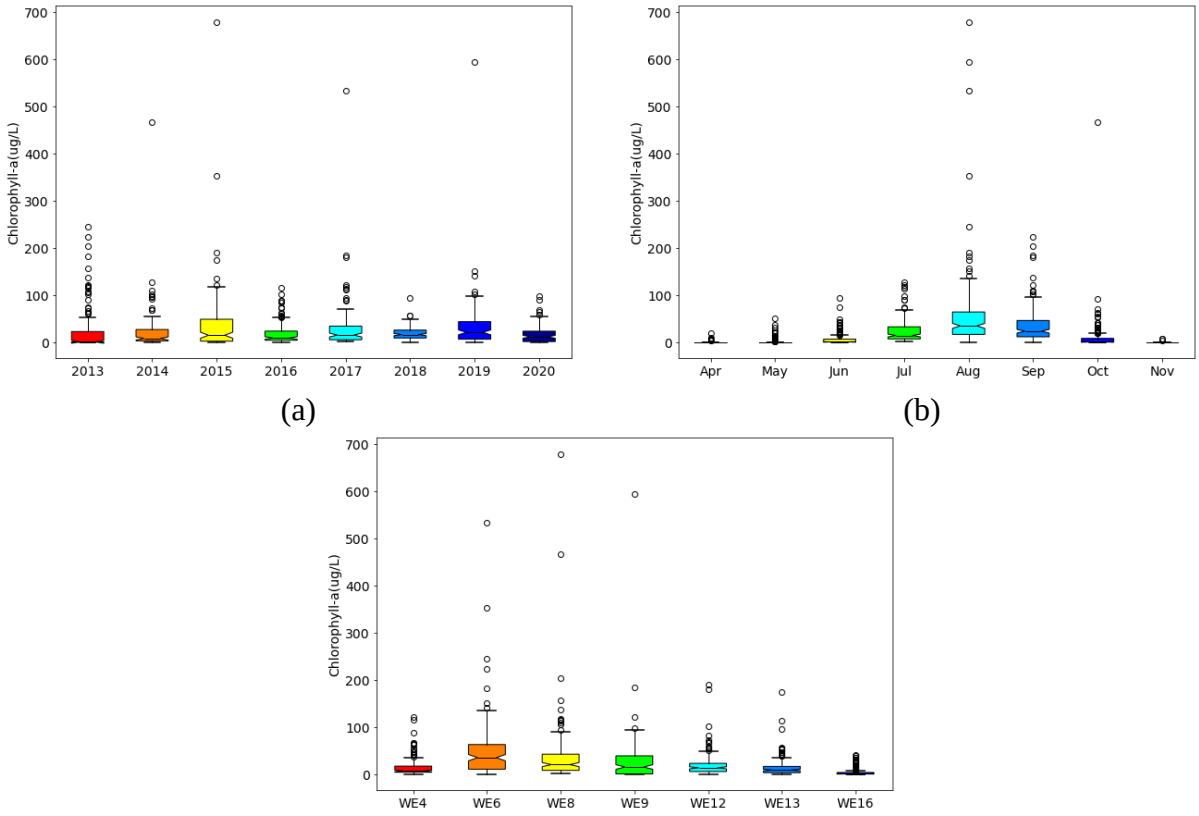

Figure 2. Box plot of chlorophyll-a concentrations in Lake Erie from 2013 to2020. (a) Yearly scale, (b) monthly scale, (c)station scale.

The LSTM model, while not performing as well as the Transformer and GRU models, still showed substantial improvements over the traditional regression models. The LSTM's lower performance compared to the GRU suggests that simpler architectures like GRU can sometimes achieve comparable or better results with less complexity. The traditional Ridge and Lasso regression models exhibited significantly higher errors, highlighting their limitations in capturing the complexities of environmental data. Among the regression models, Lasso outperformed Ridge across all metrics, showing better R-squared, MAE, MAPE, and NRMSE values. In summary, the results emphasize the superior performance of deep learning models, particularly the Transformer, in accurately predicting HABs. Both the GRU and LSTM models also demonstrated notable advantages over traditional approaches.

The Figure 3 presents a detailed comparison of the performance of three different models—LSTM, GRU, and Transformer—across different data subsets. The figure is organized into three rows, each dedicated to one of these models, and within each row, three scatter plots are displayed. The columns represent the different data subsets used for evaluation: the first column corresponds

to the model's performance on the training data, the second column corresponds to the model's performance on the test data, and the third column corresponds to the model's performance on the combined dataset (training and test data together).

Table 2. Performance Metrics for HAB Prediction Models

Model	R2	MAE	MAPE	NRMSE
Ridge	0.26	12.84	1.14	0.67
Lasso	0.38	11.56	1.00	0.61
LSTM	0.763	6.099	0.399	0.38
GRU	0.849	5.31	0.412	0.31
Transformer	0.861	5.06	0.348	0.30

In each plot, the x-axis represents the observed values, while the y-axis represents the predicted values by the model. The solid red diagonal line indicates the line of perfect agreement (1:1 line) where the model's predictions perfectly match the observed values. The blue dots (scatter points) show the actual data point, while the dotted blue line represents the best-linear fit regression line between the observed and predicted values. Across all nine plots, the alignment of the data points relative to the 1:1 line provides insight into the accuracy and bias of the models. Points that fall above the 1:1 line indicate overestimation by the model, while those below the line suggest underestimation. The closer the scatter points cluster around the perfect fit line, the better the model's predictive accuracy.

The scatter plots for the LSTM model (top row) reveal that while the LSTM can capture the overall trend of the data, there is a noticeable degree of scatter, particularly at higher concentration values for all subsets of data. This suggests that the LSTM model may struggle with predicting extreme values accurately, leading to under estimation in those cases. The GRU model (middle row) shows a slightly improved performance compared to the LSTM, with a tighter clustering of data points around the 1:1 line, particularly at moderate concentration levels and using test data.

However, similar to the LSTM, the GRU model also exhibits challenges in accurately predicting the highest concentrations, as indicated by the scatter and deviation of the regression line from the 1:1 line. The Transformer model (bottom row) demonstrates a distinct performance pattern compared to LSTM and GRU models. The scatter plots indicate that the Transformer may better handle the variability in the data, as evidenced by a closer alignment of the points with the 1:1 line, particularly at higher concentrations. This suggests that the Transformer model might be more robust in capturing the complex relationships in the dataset, leading to more accurate predictions across the full range of observed chlorophyll-a concentrations.

To further evaluate the performance of the deep learning models, predictions for the peak HAB months of July, August, and September were analyzed separately as shown in Figure 4. These months are critical as they typically exhibit the highest HAB values, particularly in August (Tewari et al., 2022). In July, the GRU model demonstrated superior performance with the lowest errors and highest R-squared value. The Transformer model also showed strong results, despite having

slightly higher errors compared to the GRU. The LSTM model had the highest errors, indicating lower predictive accuracy for this month.

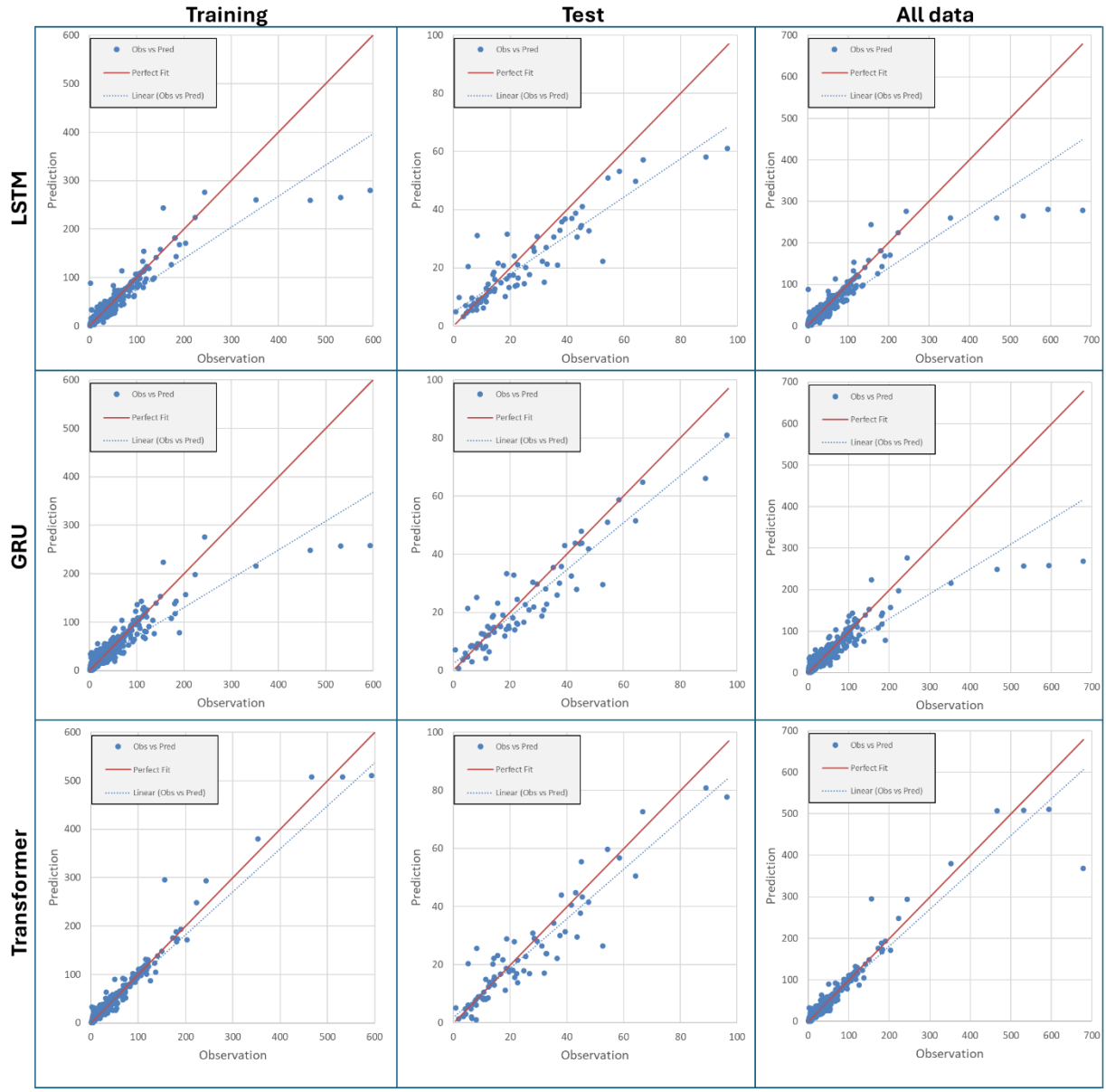

Figure 3. Scatter plots of observed chlorophyll-a concentration (x-axis) versus prediction chlorophyll-a concentration (y-axis) for deep learning models (LSTM, GRU, and Transformer by using different data subsets (training, test and all data).

During August, when HAB values peaked, the Transformer model excelled, achieving the highest accuracy among the models. The GRU model maintained strong predictive capabilities but had somewhat higher errors in comparison to the Transformer. The LSTM model improved from its July performance but still did not match the accuracy of the Transformer and GRU. In September, the Transformer model once again led in performance, with the lowest errors and

highest R-squared value. The GRU model continued to show robust predictive power, though its errors were marginally higher than those of the Transformer. The LSTM model, while better than its July performance, remained the least accurate among the deep learning models.

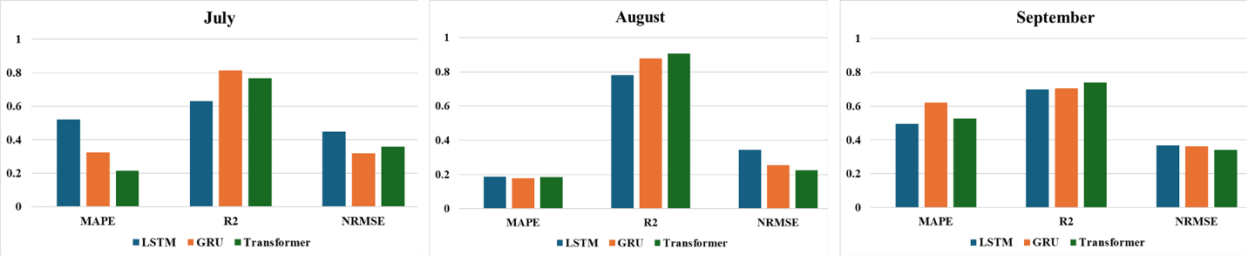

Figure 4. HABs prediction performance of tested models in peak months

Overall, the monthly analysis highlights the consistent strength of the GRU and Transformer models in predicting HABs, with the Transformer model particularly excelling during the peak month of August and maintaining top performance in September. The LSTM model, although improved, generally exhibited higher errors, suggesting that the GRU and Transformer models are better suited for capturing the dynamics of HABs in Lake Erie during these critical months.

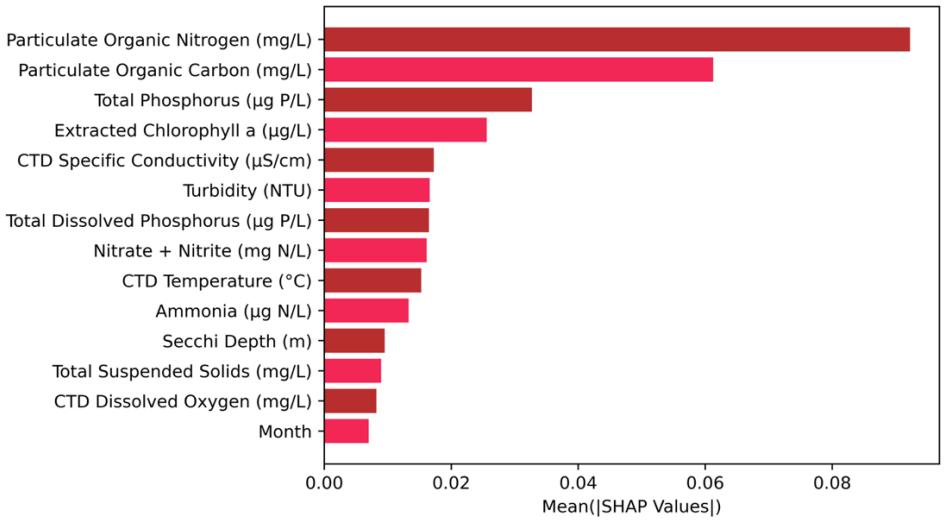

Figure 5. Feature importance analysis for Transformer model

The use of SHAP analysis can enhance the interpretability of these models, providing a deeper understanding of the key water quality parameters influencing the predictions. This interpretability supports more informed ecological management decisions, highlighting the practical applicability of these advanced models in real-world environmental monitoring and decision-making. To better understand the underlying key factors that affect the models, we performed feature importance analysis using the SHAP library.

The feature importance plot (Figure 5) for the Transformer model ranks the input variables based on their mean absolute SHAP values, highlighting the most critical factors influencing the

model's predictions. Particulate Organic Nitrogen (PON), Particulate Organic Carbon (POC), and Total Phosphorus (TP) emerge as the top three features. The significant difference in the mean SHAP value for PON compared to other factors indicates its dominant role in affecting Chlorophyll-a concentrations. This finding suggests that variations in PON have a substantial impact on the dynamics of Chlorophyll-a, potentially due to its role in nutrient cycling and algal growth (Wang et al., 2017; Du et al., 2022).

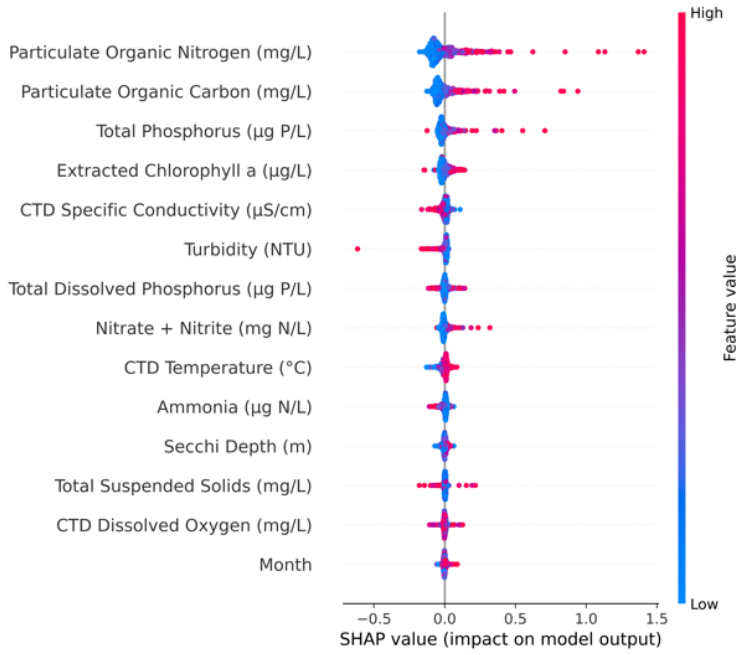

Figure 6. SHAP values of features and their impact on predictions for Transformer model

The SHAP values plot (Figure 6) for the Transformer model offers a more granular view, showing the individual SHAP values for each feature along with the corresponding feature values. Higher values of POC and PON, indicated by the red color, are associated with increased Chlorophyll-a concentrations, demonstrating a positive correlation with harmful algal bloom occurrence. In contrast, lower values, shown in blue, are linked to decreased Chlorophyll-a levels. Additionally, the SHAP analysis reveals that TP also plays a significant role in the model's predictions. High levels of TP contribute positively to Chlorophyll-a concentrations, highlighting its importance as a nutrient that supports algal growth. This aligns with ecological understanding, as phosphorus is a key nutrient that often limits primary productivity in aquatic systems (Havens et al., 2003; Zhang et al., 2024).

The GRU model, similar to the Transformer model, highlighted the significance of several key water quality parameters in predicting Chlorophyll-a concentrations. The SHAP analysis (Figures A1 and A2) for the GRU model indicates that POC, PON, and TP are the most influential features. These parameters consistently showed high mean absolute SHAP values, emphasizing their critical role in the model's predictions. Higher values of POC and PON were associated with increased

Chlorophyll-a concentrations, suggesting a positive correlation with HAB occurrence. Additionally, other features such as historical Chlorophyll-a and Nitrate + Nitrite also contributed significantly to the model's output, reinforcing the importance of nutrient levels in driving algal blooms (Rosales et al., 2022; Lee et al., 2022). The GRU model's SHAP values plot demonstrated a similar pattern to the Transformer model, with higher nutrient levels pushing the predictions towards higher Chlorophyll-a concentrations.

The LSTM model's SHAP analysis (Figures A3 and A4) further confirms the importance of certain water quality parameters in predicting Chlorophyll-a concentrations. POC, PON, and historical Chlorophyll-a emerged as the top contributing features, with consistently high mean absolute SHAP values. This finding underscores the role of particulate organic matter and phosphorus in influencing algal growth and bloom dynamics. Higher values of these features were positively correlated with increased Chlorophyll-a concentrations, indicating their significant impact on HAB events. Additionally, the LSTM model highlighted the importance of other features such as TP and Nitrate + Nitrite, which also played a crucial role in the predictions. The SHAP values plot for the LSTM model revealed that higher levels of these nutrients consistently led to higher predicted Chlorophyll-a concentrations, mirroring the patterns observed in both the Transformer and GRU models. This consistency across models reinforces the importance of these key parameters in the context of HAB forecasting.

The Transformer model distinctly outperforms its counterparts—LSTM, GRU, Ridge, and Lasso—in predicting HABs in Lake Erie. The comprehensive analyses, encapsulated in tables and figures provided throughout this section, consistently highlight the superior performance of the Transformer model. Notably, its ability to achieve higher R-squared values, along with lower MAE, MAPE, and NRMSE, underscores its robustness and precision in forecasting Chlorophyll-a concentrations. Overall, the SHAP analysis for different models consistently identifies POC, PON, and TP as the most critical features influencing the predictions of Chlorophyll-a concentrations and HABs. This consistency underscores the importance of these parameters in the context of HAB prediction. The insights provided by the SHAP methodology not only enhance the interpretability of the models but also support more informed decision-making in environmental management and public health.

5. Conclusion

In this study, we proposed a comprehensive analysis of deep learning methods for predicting chlorophyll-a concentrations, representing a significant shift from traditional methods by developing a model capable of providing integrated predictions across multiple monitoring stations rather than focusing on single-location predictions or satellite imagery. Our approach utilized comprehensive datasets encompassing physical, chemical, and biological water quality parameters from multiple monitoring stations in the western basin of Lake Erie for eight years (2013-2020). We have explored the effectiveness of advanced deep learning models, particularly the Transformer model, for predicting Chlorophyll-a concentrations within the western basin of Lake

Erie. The analysis emphasized the importance of an explainable AI approach to enhance model transparency and decision-making for ecological management.

Our comprehensive analysis, utilizing four key metrics—R-squared, MAE, MAPE, and NRMSE—demonstrates the superior capability of the Transformer model in HAB prediction. The Transformer model outperformed the LSTM, GRU, Ridge, and Lasso models, achieving higher R-squared values and lower MAE, MAPE, and NRMSE scores, thereby underscoring its precision and reliability in forecasting Chlorophyll-a concentrations. Moreover, SHAP analysis provided a reasonable interpretation of how each variable affects the HAB prediction. By using SHAP values, the effect of each variable on Chlorophyll-a prediction could be interpreted more specifically. Our analysis revealed key water quality parameters significantly influencing the HAB formation, such as Particulate Organic Carbon (POC), Particulate Organic Nitrogen (PON), and Total Phosphorus (TP).

Our analysis also included a correlation between increases in these factors and rising Chlorophyll-a concentration, which served as an indicator for HABs, highlighting a potential link that warrants further investigation This consistency underscores the importance of these parameters in the context of HAB prediction and supports more informed decision-making in ecological management and public safety. This study not only highlights the efficacy of the Transformer model in HAB prediction but also contributes significantly to the field of environmental modeling by showing the potential of advanced deep learning techniques to enhance prediction accuracy and interpretability. The integration of explainable AI methodologies ensures that the model's predictions are transparent and actionable, facilitating better management strategies for mitigating the impacts of HABs.

While the overall prediction performance provided valuable insights, it is important to acknowledge certain limitations within our study. The model was constructed using only limited number of stations owing to the missing value of data and the training period was relatively short. Further studies should develop larger benchmark dataset and extend the scope of the studies by preserving the data collected daily through continuous data management. Benchmark datasets are crucial for ensuring the reproducibility of research and facilitating the improvement of modeling studies by providing a standardized basis for comparison and validation (Demir et al., 2022; Sit et al., 2021b).

Furthermore, parameters including meteorological data such as air temperature, wind speed, precipitation, solar irradiance and hydrodynamic data such as water level, flowrate can be added to properly perform training to improve prediction performance. In addition, further development and refinement of the model's architecture and training process could also enhance its predictive capabilities. Such advancements will be crucial for improving environmental monitoring and management strategies, ultimately contributing to the sustainability of aquatic ecosystems in the face of evolving environmental challenges.

6. Acknowledgements

We would like to special thanks to Next Generation Internet Transatlantic Fellowship Program for their generous support and funding, which has been instrumental in the completion of this work.

7. References

Ai, H., Zhang, K., Sun, J., & Zhang, H. (2023). Short-term Lake Erie algal bloom prediction by classification and regression models. Water Research, 232, 119710.

Arrieta, A. B., Díaz-Rodríguez, N., Del Ser, J., Bennetot, A., Tabik, S., Barbado, A., ... & Herrera, F. (2020). Explainable Artificial Intelligence (XAI): Concepts, taxonomies, opportunities and challenges toward responsible AI. Information fusion, 58, 82-115.

Baek, S. S., Kwon, Y. S., Pyo, J., Choi, J., Kim, Y. O., & Cho, K. H. (2021). Identification of influencing factors of A. catenella bloom using machine learning and numerical simulation. Harmful Algae, 103, 102007.

Bayar, S., Demir, I., & Engin, G. O. (2009). Modeling leaching behavior of solidified wastes using back-propagation neural networks. *Ecotoxicology and environmental safety*, *72*(3), 843-850.

Baydaroğlu, Ö., Yeşilköy, S., Dave, A., Linderman, M., Demir, I. (2024). Modeling of Harmful Algal Bloom Dynamics and the Model-Based Interactive Framework for Inland Waters. EarthArxiv, 7075. https://doi.org/10.31223/X5S40X.

Baydaroğlu, Ö., & Demir, I. (2024). Temporal and spatial satellite data augmentation for deep learning-based rainfall nowcasting. Journal of Hydroinformatics, 26(3), 589-607.

Beck, M.B., Jiang, F., Shi, F., Walker, R.V., Osidele, O.O., Lin, Z., Demir, I. and Hall, J.W., (2010), March. Re-engineering cities as forces for good in the environment. In Proceedings of the institution of civil engineers-engineering sustainability, Vol. 163, No. 1, pp. 31-46.

Boegehold, A. G., Burtner, A. M., Camilleri, A. C., Carter, G., DenUyl, P., Fanslow, D., Fyffe Semenyuk, D., Godwin, C. M., Gossiaux, D., Johengen, T. H., Kelchner, H., Kitchens, C., Mason, L. A., McCabe, K., Palladino, D., Stuart, D., Vanderploeg, H., and Errera, R. (2023). Routine monitoring of western Lake Erie to track water quality changes associated with cyanobacterial harmful algal blooms. Earth System Science Data Discussions, 2023, 1-39.

Boyer, J. N., Kelble, C. R., Ortner, P. B., & Rudnick, D. T. (2009). Phytoplankton bloom status: Chlorophyll a biomass as an indicator of water quality condition in the southern estuaries of Florida, USA. Ecological indicators, 9(6), S56-S67.

Bui, H. H., Ha, N. H., Nguyen, T. N. D., Nguyen, A. T., Pham, T. T. H., Kandasamy, J., & Nguyen, T. V. (2019). Integration of SWAT and QUAL2K for water quality modeling in a data scarce basin of Cau River basin in Vietnam. Ecohydrology & Hydrobiology, 19(2), 210-223.

Buratti, F. M., Manganelli, M., Vichi, S., Stefanelli, M., Scardala, S., Testai, E., and Funari, E. (2017). Cyanotoxins: producing organisms, occurrence, toxicity, mechanism of action and human health toxicological risk evaluation, Arch. Toxicol., 91, 1049-1130.

Burkart, N., & Huber, M. F. (2021). A survey on the explainability of supervised machine learning. Journal of Artificial Intelligence Research, 70, 245-317.

Busari, I., Sahoo, D., Harmel, R. D., & Haggard, B. E. (2023). A Review of Machine Learning Models for Harmful Algal Bloom Monitoring in Freshwater Systems. Journal of Natural Resources and Agricultural Ecosystems. 1(2): 63-76.

Busari, I., Sahoo, D., Harmel, R. D., & Haggard, B. E. (2024). Prediction Of Chlorophyll-a As an Index of Harmful Algal Blooms Using Machine Learning Models. Journal of Natural Resources and Agricultural Ecosystems, 2(2), 53-61

Carmichael, W. W. and Boyer, G. L. (2016). Health impacts from cyanobacteria harmful algae blooms: Implications for the North American Great Lakes, Harmful Algae, 54, 194-212.

Castelvecchi, D. (2016). Can we open the black box of AI?. Nature News, 538(7623), 20.

Chen, X., Fu, Y., & Zhou, H. (2023). An approach of multi-element fusion method for harmful algal blooms prediction. Environmental Science and Pollution Research, 30(11), 32083-32094.

Cheng, K. H., Chan, S. N., & Lee, J. H. (2020). Remote sensing of coastal algal blooms using unmanned aerial vehicles (UAVs). Marine Pollution Bulletin, 152, 110889.

Cho, K., Van Merriënboer, B., Gulcehre, C., Bahdanau, D., Bougares, F., Schwenk, H., & Bengio, Y. (2014). Learning phrase representations using RNN encoder-decoder for statistical machine translation. arXiv preprint arXiv:1406.1078.

Demir, I., & Beck, M. B. (2009). GWIS: a prototype information system for Georgia watersheds. In Georgia Water Resources Conference: Regional Water Management Opportunities, UGA, Athens, GA, US.

Demir, I., Jiang, F., Walker, R. V., Parker, A. K., & Beck, M. B. (2009). Information systems and social legitimacy scientific visualization of water quality. In *2009 IEEE International Conference on Systems, Man and Cybernetics* (pp. 1067-1072). IEEE.

Demir, I., Xiang, Z., Demiray, B., & Sit, M. (2022). Waterbench: a large-scale benchmark dataset for data-driven streamflow forecasting. *Earth System Science Data Discussions*, *2022*, 1-19.

Demiray, B. Z., Sit, M., & Demir, I. (2023). EfficientTempNet: Temporal Super-Resolution of Radar Rainfall. arXiv preprint arXiv:2303.05552.

Demiray, B. Z., Sit, M., & Demir, I. (2021). DEM super-resolution with efficientNetV2. arXiv preprint arXiv:2109.09661.

Demiray, B. Z., Sit, M., Mermer, O., & Demir, I. (2024). Enhancing hydrological modeling with transformers: a case study for 24-h streamflow prediction. Water Science & Technology, 89(9), 2326-2341.

Demiray, B. Z., & Demir, I. (2024). Towards Generalized Hydrological Forecasting using Transformer Models for 120-Hour Streamflow Prediction. arXiv preprint arXiv:2406.07484.

Derot, J., Yajima, H., Jacquet, S. (2020) Advances in forecasting harmful algal blooms using machine learning models: A case study with Planktothrix rubescens in Lake Geneva. Harmful Algae, 99, 101906.

Du, Y., An, S., He, H., Wen, S., Xing, P., & Duan, H. (2022). Production and transformation of organic matter driven by algal blooms in a shallow lake: Role of sediments. Water Research, 219, 118560.

Franks, P. J. (2018). Recent advances in modelling of harmful algal blooms. Global ecology and oceanography of harmful algal blooms, 359-377.

Giere, J., Riley, D., Nowling, R. J., McComack, J., & Sander, H. (2020). An investigation on machine-learning models for the prediction of cyanobacteria growth. Fundamental and Applied Limnology, 194(2), 85-94.

Glibert, P. M. (2020). Harmful algae at the complex nexus of eutrophication and climate change. Harmful algae, 91, 101583.

Goodman, B., & Flaxman, S. (2017). European Union regulations on algorithmic decision-making and a "right to explanation". AI magazine, 38(3), 50-57.

Graham, J. L., Dubrovsky, N. M., & Eberts, S. M. (2016). Cyanobacterial harmful algal blooms and US Geological Survey science capabilities. US Department of the Interior, US Geological Survey.

Greene, S. B. D., LeFevre, G. H., & Markfort, C. D. (2021). Improving the spatial and temporal monitoring of cyanotoxins in Iowa lakes using a multiscale and multi-modal monitoring approach. Science of the Total Environment, 760, 143327.

Greer, B., McNamee, S. E., Boots, B., Cimarelli, L., Guillebault, D., Helmi, K., ... & Campbell, K. (2016). A validated UPLC–MS/MS method for the surveillance of ten aquatic biotoxins in European brackish and freshwater systems. Harmful algae, 55, 31-40.

Hartshorn, N., Marimon, Z., Xuan, Z., Cormier, J., Chang, N. B., & Wanielista, M. (2016). Complex interactions among nutrients, chlorophyll-a, and microcystins in three stormwater wet detention basins with floating treatment wetlands. Chemosphere, 144, 408-419.

Havens, K. E. (2003). Phosphorus–algal bloom relationships in large lakes of south Florida: implications for establishing nutrient criteria. Lake and Reservoir Management, 19(3), 222-228.

Hochreiter, S., & Schmidhuber, J. (1997). Long short-term memory. Neural computation, 9(8), 1735-1780.

Hoerl, A. E., & Kennard, R. W. (1970). Ridge regression: Biased estimation for nonorthogonal problems. Technometrics, 12(1), 55-67.

Hollister, J. W., & Kreakie, B. J. (2016). Associations between chlorophyll-a and various microcystin health advisory concentrations. F1000Research, 5.

Hu, Z., Zhang, Y., Zhao, Y., Xie, M., Zhong, J., Tu, Z., & Liu, J. (2019). A water quality prediction method based on the deep LSTM network considering correlation in smart mariculture. Sensors, 19(6), 1420.

Humbert, J. F., & Fastner, J. (2016). Ecology of cyanobacteria. Handbook of cyanobacterial monitoring and cyanotoxin analysis, 9-18.

Izadi, M., Sultan, M., Kadiri, R. E., Ghannadi, A., & Abdelmohsen, K. (2021). A remote sensing and machine learning-based approach to forecast the onset of harmful algal bloom. Remote Sensing, 13(19), 3863.

Janssen, A. B., Janse, J. H., Beusen, A. H., Chang, M., Harrison, J. A., Huttunen, I., ... & Mooij, W. M. (2019). How to model algal blooms in any lake on earth. Current opinion in environmental sustainability, 36, 1-10.

Jeong, B., Chapeta, M. R., Kim, M., Kim, J., Shin, J., & Cha, Y. (2022). Machine learning-based prediction of harmful algal blooms in water supply reservoirs. Water Quality Research Journal, 57(4), 304-318.

Katin, A., Del Giudice, D., Hall, N. S., Paerl, H. W., & Obenour, D. R. (2021). Simulating algal dynamics within a Bayesian framework to evaluate controls on estuary productivity. Ecological Modelling, 447, 109497.

Kislik, C., Dronova, I., Grantham, T. E., & Kelly, M. (2022). Mapping algal bloom dynamics in small reservoirs using Sentinel-2 imagery in Google Earth Engine. Ecological Indicators, 140, 109041.

Kouakou, C. R., & Poder, T. G. (2019). Economic impact of harmful algal blooms on human health: a systematic review. Journal of water and health, 17(4), 499-516.

Kratzert, F., Klotz, D., Brenner, C., Schulz, K., & Herrnegger, M. (2018). Rainfall–runoff modelling using long short-term memory (LSTM) networks. Hydrology and Earth System Sciences, 22(11), 6005-6022.

Langer, M., Oster, D., Speith, T., Hermanns, H., Kästner, L., Schmidt, E., ... & Baum, K. (2021). What do we want from Explainable Artificial Intelligence (XAI) ?–A stakeholder perspective on XAI and a conceptual model guiding interdisciplinary XAI research. Artificial Intelligence, 296, 103473.

Lee, S., & Lee, D. (2018). Improved prediction of harmful algal blooms in four Major South Korea's Rivers using deep learning models. International journal of environmental research and public health, 15(7), 1322.

Lee, D., Kim, M., Lee, B., Chae, S., Kwon, S., & Kang, S. (2022). Integrated explainable deep learning prediction of harmful algal blooms. Technological Forecasting and Social Change, 185, 122046.

Lin, S., Pierson, D. C., & Mesman, J. P. (2023). Prediction of algal blooms via data-driven machine learning models: an evaluation using data from a well-monitored mesotrophic lake. Geoscientific Model Development, 16(1), 35-46.

Lin, T., Wang, Y., Liu, X., & Qiu, X. (2022). A survey of transformers. AI open, 3, 111-132.

Liu, P., Wang, J., Sangaiah, A. K., Xie, Y., & Yin, X. (2019). Analysis and prediction of water quality using LSTM deep neural networks in IoT environment. Sustainability, 11(7), 2058.

Liu, S. T., & Zhang, L. (2022). Surface Chaotic Theory and the Growth of Harmful Algal Bloom. In Surface Chaos and Its Applications (pp. 299-320). Singapore: Springer Nature Singapore.

Lombard, F., Boss, E., Waite, A. M., Vogt, M., Uitz, J., Stemmann, L., ... & Appeltans, W. (2019). Globally consistent quantitative observations of planktonic ecosystems. Frontiers in Marine Science, 6, 196.

Lundberg, S. M., & Lee, S. I. (2017). A unified approach to interpreting model predictions. Advances in neural information processing systems, 30.

Lundberg, S. M., Erion, G., Chen, H., DeGrave, A., Prutkin, J. M., Nair, B., ... & Lee, S. I. (2020). From local explanations to global understanding with explainable AI for trees. Nature machine intelligence, 2(1), 56-67.

Magnuson, J. J., Webster, K. E., Assel, R. A., Bowser, C. J., Dillon, P. J., Eaton, J. G., ... & Quinn, F. H. (1997). Potential effects of climate changes on aquatic systems: Laurentian Great Lakes and Precambrian Shield Region. Hydrological processes, 11(8), 825-871.

Marndi, A., & Patra, G. K. (2020). Chlorophyll prediction using ensemble deep learning technique. In Progress in Computing, Analytics and Networking: Proceedings of ICCAN 2019 (pp. 341-349). Springer Singapore.

Maze, G., Olascoaga, M. J., & Brand, L. (2015). Historical analysis of environmental conditions during Florida Red Tide. Harmful Algae, 50, 1-7.

Mellios, N. K., Moe, S. J., & Laspidou, C. (2020). Using Bayesian hierarchical modelling to capture cyanobacteria dynamics in Northern European lakes. Water Research, 186, 116356.

Paerl, H. W., Hall, N. S., & Calandrino, E. S. (2011). Controlling harmful cyanobacterial blooms in a world experiencing anthropogenic and climatic-induced change. Science of the total environment, 409(10), 1739-1745.

Paerl, H. W., & Paul, V. J. (2012). Climate change: links to global expansion of harmful cyanobacteria. Water research, 46(5), 1349-1363.

Paerl, H. W., Gardner, W. S., Havens, K. E., Joyner, A. R., McCarthy, M. J., Newell, S. E., ... & Scott, J. T. (2016). Mitigating cyanobacterial harmful algal blooms in aquatic ecosystems impacted by climate change and anthropogenic nutrients. Harmful Algae, 54, 213-222.

Qian, J., Pu, N., Qian, L., Xue, X., Bi, Y., & Norra, S. (2023). Identification of driving factors of algal growth in the South-to-North Water Diversion Project by Transformer-based deep learning. Water Biology and Security, 2(3), 100184.

Qiu, Y., Liu, H., Liu, F., Li, D., Liu, C., Liu, W., ... & Duan, H. (2023). Development of a collaborative framework for quantitative monitoring and accumulation prediction of harmful algal blooms in nearshore areas of lakes. Ecological Indicators, 156, 111154.

Ratté-Fortin, C., Plante, J. F., Rousseau, A. N., & Chokmani, K. (2023). Parametric versus nonparametric machine learning modelling for conditional density estimation of natural events: Application to harmful algal blooms. Ecological Modelling, 482, 110415.

Rolim, S. B. A., Veettil, B. K., Vieiro, A. P., Kessler, A. B., & Gonzatti, C. (2023). Remote sensing for mapping algal blooms in freshwater lakes: A review. Environmental Science and Pollution Research, 30(8), 19602-19616.

Rosales, D., Ellett, A., Jacobs, J., Ozbay, G., Parveen, S., & Pitula, J. (2022). Investigating the Relationship between nitrate, total dissolved nitrogen, and phosphate with abundance of pathogenic Vibrios and harmful algal blooms in Rehoboth Bay, Delaware. Applied and Environmental Microbiology, 88(14), e00356-22.

Rostam, N. A. P., Malim, N. H. A. H., Azmee, N. A., Figueiredo, R. J., Osman, M. A., & Abdullah, R. (2023). Harmful algal blooms (HAB) open issues: A review of ecological data challenges,

factor analysis and prediction approaches using data-driven method. Computing and Artificial Intelligence, 1(1), 100.

Saeed, W., & Omlin, C. (2023). Explainable AI (XAI): A systematic meta-survey of current challenges and future opportunities. Knowledge-Based Systems, 263, 110273.

Shin, C. M., Kim, D., & Song, Y. (2019). Analysis of hydraulic characteristics of Yeongsan River and estuary using EFDC model. Journal of Korean Society on Water Environment, 35(6), 580-588.

Sit, M., Demiray, B., & Demir, I. (2021a). Short-term hourly streamflow prediction with graph convolutional gru networks. *arXiv preprint arXiv:2107.07039*.

Sit, M., Seo, B. C., & Demir, I. (2021b). Iowarain: A statewide rain event dataset based on weather radars and quantitative precipitation estimation. *arXiv preprint arXiv:2107.03432*.

Sit, M., Demiray, B. Z., & Demir, I. (2022). A systematic review of deep learning applications in streamflow data augmentation and forecasting. EarthArxiv, 3617. https://doi.org/10.31223/X5HM08

Sit, M., Seo, B. C., Demiray, B., & Demir, I. (2024). EfficientRainNet: Leveraging EfficientNetV2 for memory-efficient rainfall nowcasting. Environmental Modelling & Software, 106001.

Sterner, R. W., Keeler, B., Polasky, S., Poudel, R., Rhude, K., and Rogers, M. (2020). Ecosystem services of Earth's largest freshwater lakes, Ecosyst. Serv., 41, 101046.

Stubblefield, J., Hervert, M., Causey, J. L., Qualls, J. A., Dong, W., Cai, L., ... & Huang, X. (2020). Transfer learning with chest X-rays for ER patient classification. Scientific reports, 10(1), 20900.

Stumpf, R. P., Johnson, L. T., Wynne, T. T., & Baker, D. B. (2016). Forecasting annual cyanobacterial bloom biomass to inform management decisions in Lake Erie. Journal of Great Lakes Research, 42(6), 1174-1183.

Tanir, T., Yildirim, E., Ferreira, C. M., & Demir, I. (2024). Social vulnerability and climate risk assessment for agricultural communities in the United States. Science of The Total Environment, 908, 168346.

Tewari, M., Kishtawal, C. M., Moriarty, V. W., Ray, P., Singh, T., Zhang, L., ... & Tewari, K. (2022). Improved seasonal prediction of harmful algal blooms in Lake Erie using large-scale climate indices. Communications Earth & Environment, 3(1), 195.

Tibshirani, R. (1996). Regression shrinkage and selection via the lasso. Journal of the Royal Statistical Society: Series B (Methodological), 58(1), 267-288.

Tounsi, A., Abdelkader, M., & Temimi, M. (2023). Assessing the simulation of streamflow with the LSTM model across the continental United States using the MOPEX dataset. Neural Computing and Applications, 35(30), 22469-22486.

Vaswani, A., Shazeer, N., Parmar, N., Uszkoreit, J., Jones, L., Gomez, A. N., ... & Polosukhin, I. (2017). Attention is all you need. Advances in neural information processing systems, 30.

Verhamme, E. M., Redder, T. M., Schlea, D. A., Grush, J., Bratton, J. F., & DePinto, J. V. (2016). Development of the Western Lake Erie Ecosystem Model (WLEEM): Application to connect

phosphorus loads to cyanobacteria biomass. Journal of Great Lakes Research, 42(6), 1193-1205.

Wang, G., Zhou, W., Cao, W., Yin, J., Yang, Y., Sun, Z., ... & Zhao, J. (2011). Variation of particulate organic carbon and its relationship with bio-optical properties during a phytoplankton bloom in the Pearl River estuary. Marine pollution bulletin, 62(9), 1939-1947.

Wang, P., Yao, J., Wang, G., Hao, F., Shrestha, S., Xue, B., ... & Peng, Y. (2019). Exploring the application of artificial intelligence technology for identification of water pollution characteristics and tracing the source of water quality pollutants. Science of the Total Environment, 693, 133440.

Weirich, C. A., & Miller, T. R. (2014). Freshwater harmful algal blooms: toxins and children's health. Current problems in pediatric and adolescent health care, 44(1), 2-24.

Wells, M. L., Trainer, V. L., Smayda, T. J., Karlson, B. S., Trick, C. G., Kudela, R. M., ... & Cochlan, W. P. (2015). Harmful algal blooms and climate change: Learning from the past and present to forecast the future. Harmful algae, 49, 68-93.

Wells, M. L., Karlson, B., Wulff, A., Kudela, R., Trick, C., Asnaghi, V., ... & Trainer, V. L. (2020). Future HAB science: Directions and challenges in a changing climate. Harmful algae, 91, 101632.

Wool, T., Ambrose Jr, R. B., Martin, J. L., & Comer, A. (2020). WASP 8: The next generation in the 50-year evolution of USEPA's water quality model. Water, 12(5), 1398.

Wu, H., Xu, J., Wang, J., & Long, M. (2021). Autoformer: Decomposition transformers with auto-correlation for long-term series forecasting. Advances in Neural Information Processing Systems, 34, 22419-22430.

Wynne, T. T., Stumpf, R. P., Tomlinson, M. C., Fahnenstiel, G. L., Dyble, J., Schwab, D. J., & Joshi, S. J. (2013). Evolution of a cyanobacterial bloom forecast system in western Lake Erie: Development and initial evaluation. Journal of Great Lakes Research, 39, 90-99.

Yan, Z., Kamanmalek, S., & Alamdari, N. (2024a). Predicting coastal harmful algal blooms using integrated data-driven analysis of environmental factors. Science of The Total Environment, 912, 169253.

Yan, Z., Kamanmalek, S., Alamdari, N., & Nikoo, M. R. (2024b). Comprehensive Insights into Harmful Algal Blooms: A Review of Chemical, Physical, Biological, and Climatological Influencers with Predictive Modeling Approaches. Journal of Environmental Engineering, 150(4), 03124002.

Yeşilköy, S., & Demir, I. (2024). Crop yield prediction based on reanalysis and crop phenology data in the agroclimatic zones. Theoretical and Applied Climatology, 1-14.

Yu, P., Gao, R., Zhang, D., & Liu, Z. P. (2021). Predicting coastal algal blooms with environmental factors by machine learning methods. Ecological Indicators, 123, 107334.

Zhang, X., Li, Y., Zhao, J., Wang, Y., Liu, H., & Liu, Q. (2024). Temporal dynamics of the Chlorophyll a-Total phosphorus relationship and algal production efficiency: Drivers and management implications. Ecological Indicators, 158, 111339.

Zhang, Z., Zhang, S., Chen, C., & Yuan, J. (2024). A systematic survey of air quality prediction based on deep learning. Alexandria Engineering Journal, 93, 128-141.

Zheng, L., Wang, H., Liu, C., Zhang, S., Ding, A., Xie, E., ... & Wang, S. (2021). Prediction of harmful algal blooms in large water bodies using the combined EFDC and LSTM models. Journal of Environmental Management, 295, 113060.

Zhou, Z. X., Yu, R. C., & Zhou, M. J. (2017). Resolving the complex relationship between harmful algal blooms and environmental factors in the coastal waters adjacent to the Changjiang River estuary. Harmful Algae, 62, 60-72.

Zhou, H., Zhang, S., Peng, J., Zhang, S., Li, J., Xiong, H., & Zhang, W. (2021, May). Informer: Beyond efficient transformer for long sequence time-series forecasting. In Proceedings of the AAAI conference on artificial intelligence (Vol. 35, No. 12, pp. 11106-11115).

Zhou, Z. X., Yu, R. C., & Zhou, M. J. (2022a). Evolution of harmful algal blooms in the East China Sea under eutrophication and warming scenarios. Water Research, 221, 118807.

Zhou, T., Ma, Z., Wen, Q., Wang, X., Sun, L., & Jin, R. (2022b). Fedformer: Frequency enhanced decomposed transformer for long-term series forecasting. In International conference on machine learning (pp. 27268-27286). PMLR.

Appendix

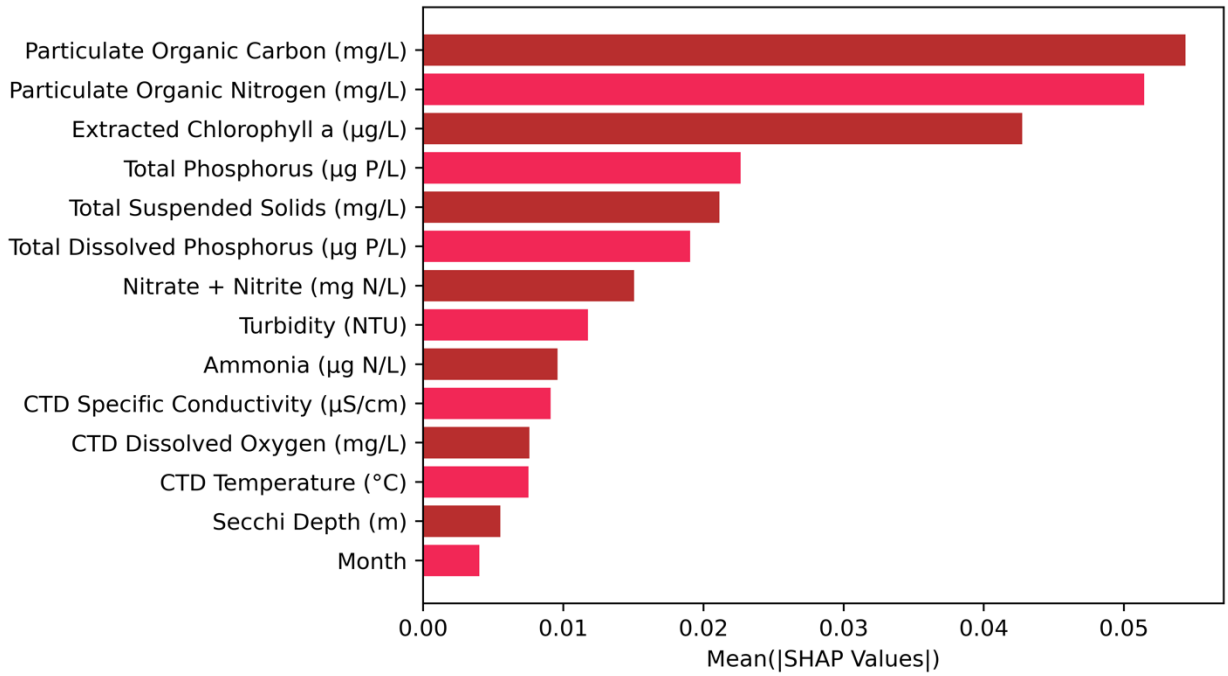

Figure A1. Feature importance analysis for GRU model

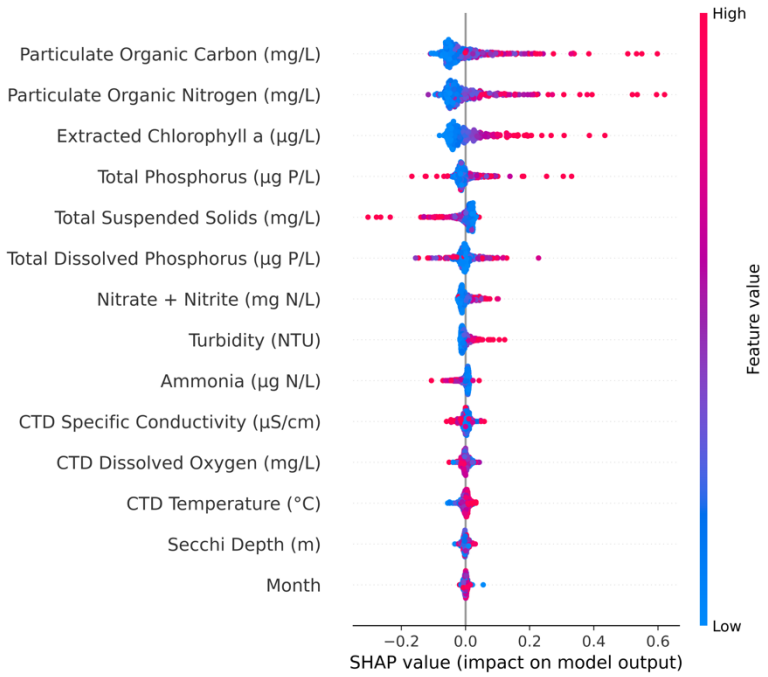

Figure A2. SHAP values of features and their impact on predictions for GRU model

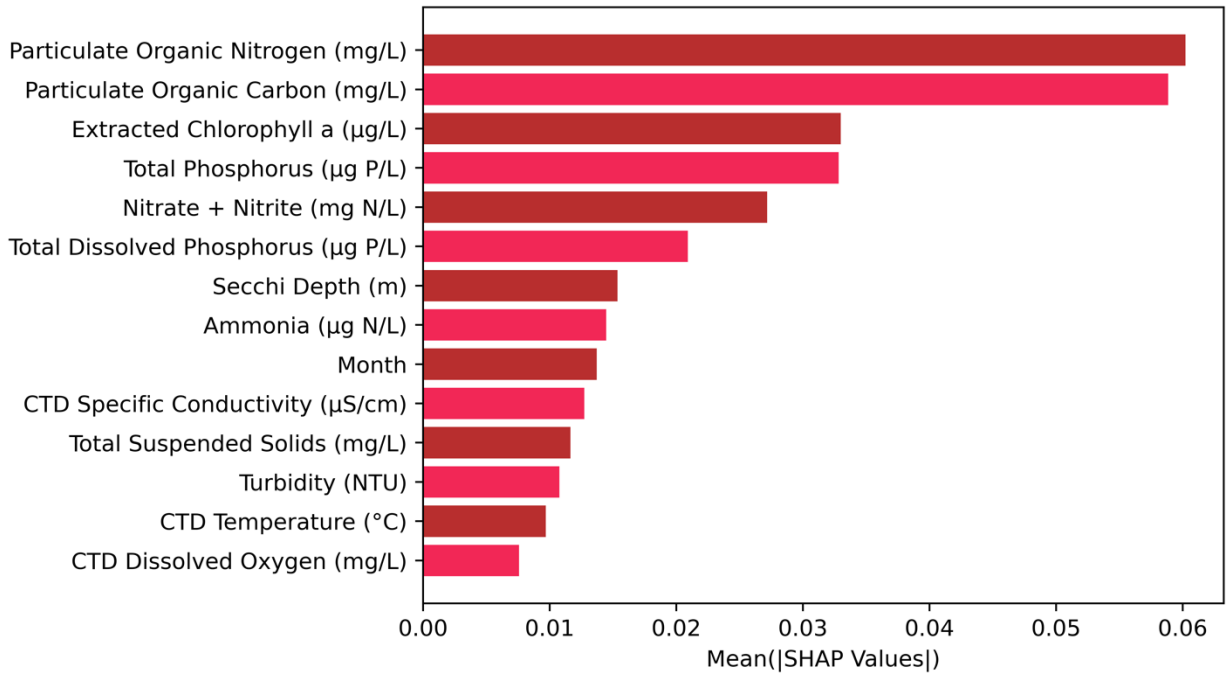

Figure A3. Feature importance analysis for LSTM model

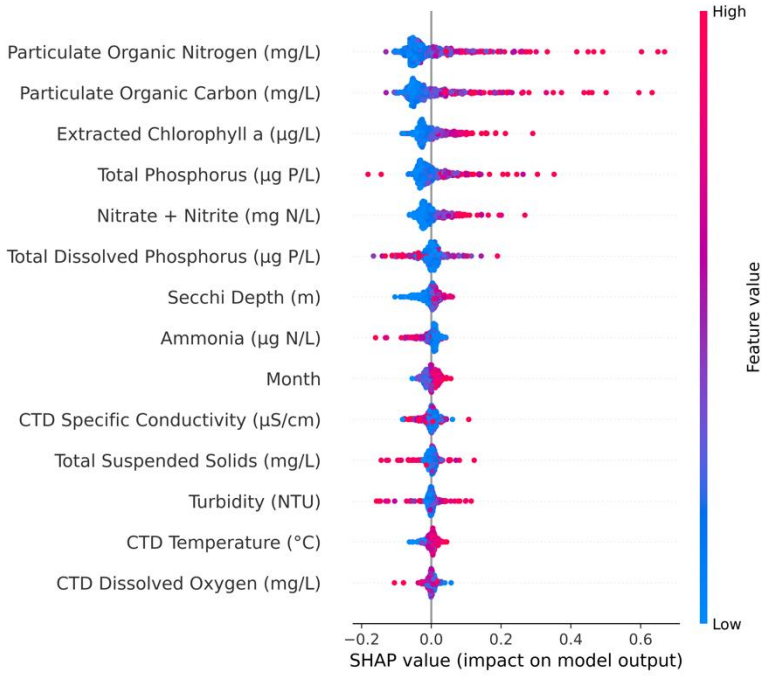

Figure A4. SHAP values of features and their impact on predictions for LSTM model